

## Tests of Gaussianity of CMB maps

Enrique Martínez-González<sup>1</sup>, R. Belén Barreiro<sup>1,2</sup>, José M. Diego<sup>1,2</sup>, José Luis Sanz<sup>1</sup>, Laura Cayón<sup>1</sup>, Joseph Silk<sup>3</sup>, Silvia Mollerach<sup>4</sup> & Vicent J. Martínez<sup>5</sup>

<sup>1</sup> *Instituto de Física de Cantabria, Consejo Superior de Investigaciones Científicas-Universidad de Cantabria, Avda. Los Castros s/n, 39005 Santander, Spain*

<sup>2</sup> *Departamento de Física Moderna, Universidad de Cantabria, Avda. Los Castros s/n, 39005 Santander, Spain*

<sup>3</sup> *Center for Particle Astrophysics, Department of Astronomy and Physics, University of California, Berkeley CA 94720-7304, USA*

<sup>4</sup> *Departamento de Física, Universidad Nacional de La Plata, cc 67, La Plata 1900, Argentina*

<sup>5</sup> *Departamento de Astronomía y Astrofísica, Universidad de Valencia, E-46100 Burjasot, Valencia, Spain*

**ABSTRACT** We study two different methods to test Gaussianity in CMB maps. One of them is based on the partition function and the other on the morphology of hot and cold spots. The partition function contains information on all the moments and scales, being a useful quantity to compress the large data sets expected from future space missions like Planck. In particular, it contains much richer information than the one available through the radiation power spectrum. The second method utilizes morphological properties of hot and cold spots such as the eccentricity and number of spots in CMB maps. We study the performance of both methods in detecting non-Gaussian features in small scale CMB simulated maps as those which will be provided by the Planck mission.

**KEYWORDS:** CMB anisotropy. Gaussianity.

### 1. INTRODUCTION

Future CMB experiments like the Planck mission will provide very large data sets at small angular scales with a high sensitivity. Their analysis will require the development of new and sophisticated methods capable of managing the data, performing an optimal separation of the different components (CMB, Galactic and extragalactic foregrounds), extracting their statistical properties and finally determining the fundamental cosmological parameters. Two methods for foreground removal have already been proposed based on Maximum Entropy (Hobson et al. 1998, 1999a) and Wiener filter (Tegmark and Efstathiou 1996). The power spectrum of the temperature fluctuations is the most widely used quantity in order to compress the data and obtain the cosmological parameters. This quantity only carries information on the second moment of the distribution and completely characterizes the statistical properties of the data if these are Gaussian distributed. However, at present there

is no experimental evidence for that statistical behaviour in the small scale temperature fluctuations. Moreover, topological defect models predict non-Gaussian temperature fluctuations. It is therefore very important to explore other quantities that can be sensitive to non-Gaussian features and can test the assumption of Gaussianity usually made for the cosmological signal.

Several studies of the Gaussian character of the CMB signal based on different statistical and morphological quantities have already been performed. They include extrema correlation function (Kogut et al. 1996, Barreiro et al. 1998), number of hot and cold spots (Coles and Barrow 1987), genus (Gott et al. 1990, Kogut et al. 1996), bispectrum (Ferreira et al. 1998, Heavens 1998), wavelets (Hobson et al. 1999b, Pando et al. 1999) and multifractals (Pompilio et al. 1995).

In this paper we concentrate on the recently proposed partition function of the CMB temperature and also on the morphology of the temperature extrema. The usefulness of the partition function to study the Gaussianity of the CMB has already been pointed out in a previous work (Diego et al. 1999). The study of morphological properties of CMB extrema, such as number, curvature and eccentricity, has been done by Barreiro et al. (1997) for Gaussian temperature fluctuations. Here we will probe the practical performance of both methods by testing their ability to find the non-Gaussian features of very weakly perturbed Gaussian random fields. In particular we will simulate small scale temperature maps by slightly perturbing Gaussian ones and generating a small: a) skewness or b) kurtosis.

## 2. TESTS OF GAUSSIANTY

### 2.1 The partition function

The partition function has recently been introduced to study CMB data by Diego et al. (1999). Below we concentrate on the application of this function to the study of Gaussianity.

The partition function is defined as follows:

$$Z(q, \delta) = \sum_{i=1}^{N_{\text{boxes}}(\delta)} \mu_i(\delta)^q \quad (1)$$

The quantity  $\mu_i(\delta)$  is called the *measure*, it is a function of  $\delta$  which is the size or scale of the boxes used to cover the sample. The boxes are labeled by  $i$  and  $N_{\text{boxes}}(\delta)$  is the number of boxes (or cells) needed to cover the map when the grid with resolution  $\delta$  is used. The exponent  $q$  is a continuous real parameter that plays the role of the order of the moment of the measure.

Let us consider a CMB map of  $N$  pixels. Now the map is divided in boxes of size  $\delta \times \delta$  pixels and the measure  $\mu_i(\delta)$  is computed in each one of the resulting boxes. Changing both,  $q$  and  $\delta$ , one calculates the function  $Z(q, \delta)$ . We would like to emphasize that the calculation of  $Z(q, \delta)$  is  $O(N)$ .

One is free to make any choice of the measure  $\mu(\delta)$  provided that several conditions

are satisfied, the most restrictive being  $\mu_i(\delta) \geq 0$ . There are no general rules to decide which is the best choice. To test Gaussianity we use the following measure:

$$\mu_i(\delta) = \frac{1}{T_*} \sum_{\text{pix}_j \in \text{box}_i} T_{\text{pix}_j}. \quad (2)$$

Thus the measure in the box  $i$  is the sum of the *absolute* temperatures  $T_{\text{pix}}$  of the pixels inside the box in units of Kelvin. The constant  $T_*$  is a normalization constant. The measures are interpreted as probabilities and they have to be normalized, i.e  $\sum_i \mu_i = 1$ . So  $T_*$  is simply the sum of the absolute temperatures over all pixels and therefore is a constant for all boxes and scales.

Summarizing,  $Z(q, \delta)$  contains information at different scales and moments. The multi-scale information gives an idea of the correlations in the map, meanwhile the moments are sensitive to possible asymmetries in the data, as well as some deviations from Gaussianity. In order to study the last property let us introduce the generating function:

$$G_\mu(q) = \langle e^{q\mu} \rangle = \frac{1}{N_{\text{boxes}}(\delta)} \sum_{i=1}^{N_{\text{boxes}}(\delta)} e^{q\mu_i(\delta)}. \quad (3)$$

Defining a new function  $H(q)$  in the following way,

$$H(q) = \ln G_\mu(q) - q\langle\mu\rangle - \frac{q^2\sigma_\mu^2}{2}, \quad (4)$$

this function vanishes for any value of  $q$  when a Gaussian distributed variable is considered. In the case of the CMB temperature, if the universe went through a phase of inflation then the fluctuations generated in the CMB will be Gaussian. However, due to the cosmic and sample variance  $H(q)$  for a given realization will not exactly vanishes, as we will see in the next section.

## 2.2 The morphology of hot and cold spots

The properties of the CMB temperature peaks for the Gaussian case have been recently studied in Barreiro et al. (1997). The local description of maxima involves the second derivatives of the field along the two principal directions. As usual, the curvature radii are defined by  $R_1 = [-\Delta_1''(\text{max})/2]^{-1/2}$  and  $R_2 = [-\Delta_2''(\text{max})/2]^{-1/2}$ , where  $\Delta$  is the temperature field normalized to the rms fluctuations. Then, we can associate two invariant quantities to any maximum: the Gaussian curvature  $\kappa$  and the eccentricity  $\epsilon$  given by

$$\kappa = \frac{1}{R_1 R_2}, \quad \epsilon = \left[ 1 - \left( \frac{R_2}{R_1} \right)^2 \right]^{1/2}. \quad (5)$$

In addition to the Gaussian curvature and the eccentricity another interesting property is the number of maxima (minima)  $N_{>\nu}$  above (below) a given temperature threshold  $\nu$  ( $-\nu$ ) in CMB maps. For symmetric distributions, such as the

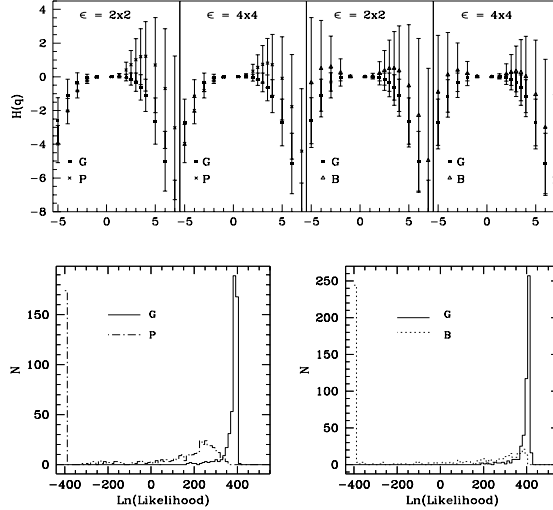


FIGURE 1. Top: The function  $H(q)$  for two different sizes of the boxes. Bottom: Distribution of  $\text{Ln}(\text{Likelihood})$  corresponding to  $H(q)$  for the Gaussian and non-Gaussian models (see text).

Gaussian one, the number of maxima and minima are statistically undistinguishable. Thus, any asymmetry present would be a mark of non-Gaussianity. Instead of using those morphological quantities for extrema in practice it is simpler to use excursion sets, i.e. hot and cold spots regions above and below a given temperature threshold. Therefore, we will count the number of excursion sets from the maps. To estimate the eccentricity of the excursion sets we fit each region (formed by at least 6 pixels) with an ellipse of equal area as the corresponding excursion set. Finally, the Gaussian curvature is a more difficult quantity to estimate from the simulated maps and we will leave it for a forthcoming paper.

### 3. SIMULATIONS

We perform small scale simulations of size  $12.8 \times 12.8$  degrees with pixel and antenna sizes similar to those of the best Planck channels, i.e.  $1'.5$  and  $5'$  respectively. The amount of instrumental noise in the maps provided by this mission is expected to be much smaller than the CMB signal, then, as a first approximation, it is not considered in this work. We simulate maps with Gaussian and non-Gaussian statistical properties, that will be used to test the previously discussed methods. The properties of the Gaussian perturbations are completely defined by the standard inflationary model. Although many models have been proposed for which non-Gaussian temperature perturbations are produced, however all their statistical

properties are either not given or are very complicated to simulate. We then consider “generic” non-Gaussian perturbations derived from Gaussian ones using transformations given by Cole and Weinberg (1992). The non-Gaussian temperature fields are derived from Gaussian fields in two ways. First, we perform the following transformation to an uncorrelated 2D Gaussian field  $G$ :  $\exp(aG) - \exp(a^2/2)$  with  $a$  a parameter which recovers the Gaussian case when  $a \rightarrow 0$ . An uncorrelated non-Gaussian field with zero mean is thus obtained. The radiation power spectrum corresponding to a standard CDM model normalized to COBE/DMR is introduced by rescaling the amplitude of each Fourier mode to that spectrum. By rescaling the power spectrum the 1-point distribution is modified with respect to the uncorrelated one, but it is still non-Gaussian. Second, we consider the transformation:  $G[\exp(aG) + \exp(-aG)]$ . Then the same radiation power spectrum is introduced as before. Finally the maps are smoothed with a FWHM=  $5'$ . In the first case we construct a non-Gaussian field whose distribution is skewed with a positive tail (P) and in the second one the distribution is broadened with both positive and negative tails (B). For both non-Gaussian fields we consider small enough values of the parameter  $a$  such that their 1-point distributions are undistinguishable from a Gaussian. In addition their power spectra are undistinguishable from the one of the Gaussian CDM model by construction.

#### 4. RESULTS

The results of comparing two sets of simulated maps, one corresponding to Gaussian fluctuations and the other to one of the previous non-Gaussian fields, using the methods described in section 2 are summarized in figures 1 and 2 for the functions  $H(q)$  and  $N_{>\nu}$ , respectively. We have considered a value  $a = 0.8$  for which it is impossible to distinguish between the corresponding 1-pdf. For the set of values of  $H(q)$  ( $N_{>\nu}$ ) given by the top of figure 1 (2) we have constructed a likelihood function whose values for each of the simulated Gaussian and non-Gaussian maps (compared to the Gaussian model) are shown in the bottom of figure 1 (2). We see that a positive result, i.e. it is possible to distinguish between the two distributions for most of the simulations, is obtained for the P non-gaussian field for both the  $H(q)$  and  $N_{>\nu}$  quantities. In the case of the B non-gaussian field the difference is less pronounced but it is still possible to discriminate between both models in a number of cases.

We have also performed a similar test for the eccentricity  $\epsilon_{>\nu}$  but in this case it is not possible to discriminate the Gaussian and any of the non-Gaussian fields.

Summarizing, the function  $H(q)$  as well as  $N_{>\nu}$  are sensitive quantities with which to probe the possible non-Gaussian features that can be present in future high sensitivity maps. On the contrary, the eccentricity is not a good discriminator of Gaussianity at least for the small maps considered in the present work.

ACKNOWLEDGMENTS This work has been supported by Spanish DGES Project PB95-1132-C02-02, Spanish CICYT Acci3n Especial ESP98-1545-E and USA-Spain Science and Technology

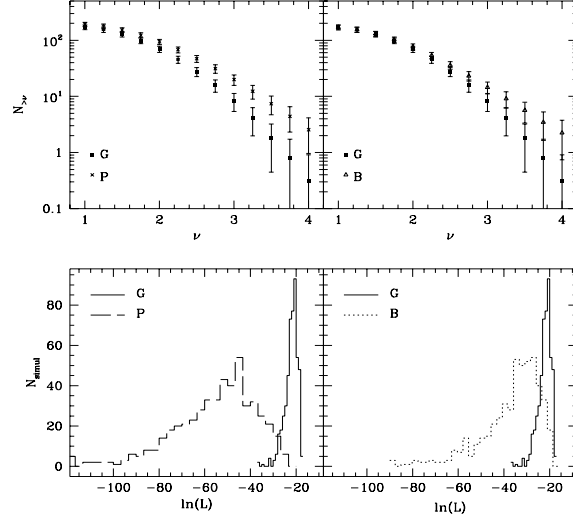


FIGURE 2. Top:  $N_{>\nu}$  for thresholds  $\nu$  in the range 1 – 4. Bottom: Distribution of  $\ln(\text{Likelihood})$  corresponding to  $N_{>\nu}$  for the Gaussian and non-Gaussian models (see text).

Program, ref. 98138. JMD and RBB have been supported by a Spanish MEC fellowship.

#### REFERENCES

- Barreiro, R.B., Sanz, J.L., Martínez-González, E., Cayón, L., Silk, J., 1997, ApJ, 478, 1.  
 Barreiro, R.B., Sanz, J.L., Martínez-González, E., Silk, J., 1998, MNRAS, 296, 693.  
 Cole, S. & Weinberg, D.H., 1992, MNRAS, 259, 652.  
 Coles, P. & Barrow, J.D., 1987, MNRAS, 228, 407.  
 Diego, J.M., Martínez-González, E., Sanz, J.L., Mollerach, S. & Martínez, V.J., 1999, MNRAS, in press (astro-ph/9902134)  
 Ferreira, P.G., Magueijo, J. & Górski, K., 1998, ApJ, 503, L1.  
 Gott III, J.R. et al., 1990, ApJ, 352, 1.  
 Heavens, A.F., 1998, astro-ph/9804222.  
 Hobson, M.P., Jones, A.W., Lasenby, A.N. & Bouchet, F.R., 1998a, MNRAS, 300, 1.  
 Hobson, M.P. et al., 1999a, MNRAS, in press (astro-ph/9810241)  
 Hobson, M.P., Jones, A.W. & Lasenby, A.N., 1999b, MNRAS, in press. (astro-ph/9810200)  
 Kogut, A. et al., 1996, 464, L29.  
 Luo, X., 1994, ApJ, 427, 71L.  
 Pando, J., Valls-Gabaud, D., Fang, L., 1998, PRL, 81, 4568.  
 Pompilio, M.P., Bouchet, F.R., Murante, G. & Provenzale, A., 1995, ApJ, 449, 1  
 Tegmark, M. & Efstathiou, G., 1996, MNRAS, 281, 1297.